Accepted Version of J. Phys. Chem. A 2019, 123, 1558 doi: 10.1021/acs.jpca.8b10836

This document is confidential and is proprietary to the American Chemical Society and its authors. Do not copy or disclose without written permission. If you have received this item in error, notify the sender and delete all copies.

Magnetically-Induced Current Density Spatial Domains

Journal:	*The Journal of Physical Chemistry*
Manuscript ID	jp-2018-10836b.R2
Manuscript Type:	Article
Date Submitted by the Author:	n/a
Complete List of Authors:	Monaco, Guglielmo; Universita degli Studi di Salerno, Dipatimento di Chimica e Biologia Zanasi, Riccardo; Università di Salerno, Dipartimento di Chimica e Biologia "A. Zambelli"

SCHOLARONE™
Manuscripts

The Journal of Physical Chemistry
Accepted Version of J. Phys. Chem. A 2019, 123, 1558 doi: 10.1021/acs.jpca.8b10836

Magnetically-Induced Current Density Spatial Domains

Guglielmo Monaco and Riccardo Zanasi*

Dipartimento di Chimica e Biologia "A. Zambelli", Univerità degli Studi di Salerno, via Giovanni Paolo II 132, Fisciano 84084, SA, Italy

E-mail: rzanasi@unisa.it

Phone: +0039 089 969590. Fax: +0039 089 969563

Abstract

The pseudo-stagnation graphs of the current density induced by a magnetic field perpendicular to the plane of the carbon atoms of benzene and cyclopropane, chosen as archetypal of π- and σ-aromatic molecules, have been worked out. Saddle nodes forming the saddle stagnation lines of the pseudo-stagnation graph have been connected by means of trajectories of the current density, which delimit the border of four different sectors of flow around each saddle line. The merging of all such boundary trajectories provides local zero-flux surfaces in the pseudo-current density, i.e., separatrices, which split the induced current density field in a number of three-dimensional domains of flow. As a result, a new partition scheme, corresponding to the physical flow that one could observe, has been obtained. For benzene and cyclopropane, by integration of the current density over the various spatial domains, the parallel component of the nuclear magnetic shielding and magnetizability tensors has been decomposed into contributions that are hard to reconcile with any atomic models of partition.

1 Introduction

Nearly twenty-five years ago Keith and Bader published three outstanding papers [1–3] concerning the calculation of accurate origin-independent induced molecular current densities, [1] the topological analysis of the three-dimensional vector field associated to such induced current densities [2] and the expression of the molecular magnetizability tensor as the sum of atomic contributions. [3] These papers have paved the way for a very large number of subsequent works given by many research groups.

The CSGT (continuous set of gauge transformations) method, [1] also referred to as CTOCD-DZ1 (continuous transformation of the origin of the current density - diamagnetic zero, without shifting the origin toward the nearest nucleus), [4] or *ipsocentric* approach, [5,6] has received much attention for the calculation of origin-independent current density maps in aromatic, antiaromatic and non-aromatic systems. [7,8] In parallel, molecular magnetic properties can be obtained by volume integration of the current density multiplied by an appropriate geometric factor, i.e., by integration of a property density function. [9] However, as it concerns the calculation of molecular magnetic properties, the GIAO (gauge-including atomic orbital or London orbitals [10,11]) predictions for both HF and DFT have been found to converge faster with respect to basis set size than those determined using the CSGT method, and then the latter is considered relatively less accurate than GIAO using the same basis set, [12] so that most recent work are performed using GIAOs. [13] Yet, modification of the CSGT by either a shift of the current density origin toward the nearest nucleus, as proposed again by Keith and Bader, [1] and then referred to as CTOCD-DZ2 (continuous transformation of the origin of the current density - diamagnetic zero, with shifting the origin toward the nearest nucleus) by us, or using the nuclear weight function of the Becke's algorithm, [14] greatly improve the computed nuclear magnetic shieldings. [12] Using same basis set, CTOCD-DZ2 predictions for ^{13}C shielding tensor components are generally found very close to the GIAO estimates.

The topological analysis of the magnetically-induced current density, presented by Keith and Bader in the second of their seminal papers, [2] enabled one to unambiguously locate and

The Journal of Physical Chemistry
Accepted Version of J. Phys. Chem. A 2019, 123, 1558 doi: 10.1021/acs.jpca.8b10836

classify the critical points for the full three-dimensional vector current field, thus completing and sometime correcting, within a systematic theory, previous works that were limited to the analysis of planar maps.[15–22] The recognition that the current density is a fully three-dimensional field represents an essential step to classifying and understanding the structure of such pseudo-observable.

In the third paper,[3] Bader and Keith showed how to split the magnetizability tensor into atomic contributions, each consisting of a basin and a surface component. The magnetic properties are determined by the electron current density and the atomic behaviour was correlated to the separation into atomic basins of the electron density, in conformity with the quantum theory of atoms in molecules (QTAIM).[23] Since, the basin component of an atomic contribution is given by the integral of the magnetization density over the corresponding atomic basin defined on the topology of $\boldsymbol{\nabla}\rho(\mathbf{r})$ and the surface component by the integral of the current density flux through the interatomic surfaces that the atom shares with its bonded neighbours, it has been suggested that the importance of the basin component relative to the surface component could provide a quantitative measure of the electron localization extent within an atomic basin.

In this paper we report an in-depth topological analysis of the first-order current density induced by an external magnetic field perpendicular to the plane of the carbon atoms of benzene and cyclopropane, which open the way of working out a set of surfaces of separation, hereafter referred to as separatrices (single form: separatrix), after Gomes,[19] that confine the current flow into a number of isolated molecular regions, hereafter referred to as current density domains. The parallel component of the magnetizability, ^{13}C, ^{1}H and centre of mass magnetic shielding tensors are then determined integrating the corresponding density functions over such domains of current density. Owing to the definition of separatrix, there is no surface components. As a consequence, a new partition scheme that corresponds closely to the effective physical flow is obtained, which permits to understand and quantify the contributions that different molecular regions give to the magnetic properties of the

molecule.

2 Methods

All the results hereafter presented, as well as equilibrium geometries, have been obtained at the DFT level combining the B97-2 functional[24] with the aug-cc-pVTZ basis set.[25] A discussion about the quality of the magnetic properties that can be obtained using the B97-2 functional has been reported by Flaig et al.[26]

The CTOCD-DZ2 method,[4,9,27,28] which is based on the CSGT by Keith and Bader,[1] has been used to compute the magnetically-induced, origin-independent, first-order current density. A description of the implementation of the CTOCD method at DFT level has been given by Havenith et al[29,30] and Soncini et al.[31]

Equilibrium geometries and unperturbed calculations have been performed using the Gaussian'09 package.[32] First-order coupled-perturbed Kohn-Sham (CPKS) calculations have been accomplished using the SYSMO suite of programs.[33]

2.1 Stagnation graph of the current density

This section is aimed at reviewing the stagnation graph (SG) of the current density, the notation and to describe a simplified SG, i.e., the *pseudo*-SG,[34] which provides the fundamental piece of information to build up the current density domains.

The magnetically-induced current density can be written as a perturbation expansion[7]

$$J_\alpha(\mathbf{r}) = J_\alpha^{(0)}(\mathbf{r}) + \mathcal{J}_\alpha^{B_\delta}(\mathbf{r})B_\delta + \cdots \tag{1}$$

where $\mathcal{J}_\alpha^{B_\delta}(\mathbf{r})$ is the second-rank current density tensor and $J_\alpha^{\mathbf{B}}(\mathbf{r}) = \mathcal{J}_\alpha^{B_\delta}(\mathbf{r})B_\delta$ is the first-order current density. Since the interest here is only on the linear response for system having a vanishing intrinsic current density, hereafter the magnetically-induced, first-order current density will be briefly referred to as current density.

Accepted Version of J. Phys. Chem. A 2019, 123, 1558 doi: 10.1021/acs.jpca.8b10836

The current density $\mathbf{J^B} = \mathbf{J^B}(\mathbf{r})$ is a three-dimensional vector field, which can be represented in various ways, for example by means of separated maps of trajectories and moduli[17] or by using oriented arrows of size proportional to its magnitude.[35,36] Perhaps, the most convenient and compact way to represent $\mathbf{J^B}$ is by using the so called stagnation graph of the current density.[18,19] The SG shows the isolated points and the lines at which the current density vector field vanishes. Points where the field is non-zero are called regular; points where it vanishes are the singular points of the field. The singularities determine the topological structure of the vector field.[2]

The field $\mathbf{J^B}(\mathbf{r})$ in the vicinity of a singularity at $\mathbf{r}_0$ can be described as the truncated Taylor series expansion

$$J^{\mathbf{B}}_{\alpha}(\mathbf{r}) = (r_\beta - r_{0\beta}) \left(\nabla_\beta J^{\mathbf{B}}_{\alpha}\right)_{\mathbf{r}_0} + \frac{1}{2}(r_\beta - r_{0\beta})(r_\gamma - r_{0\gamma}) \left(\nabla_\beta \nabla_\gamma J^{\mathbf{B}}_{\alpha}\right)_{\mathbf{r}_0} + \cdots , \qquad (2)$$

where the standard tensor notation is employed and, according to the Einstein convention, the summation over repeated Greek indices is implied. The 3×3 Jacobian matrix $\left(\nabla_\beta J^{\mathbf{B}}_{\alpha}\right)_{\mathbf{r}_0}$, evaluated at the stagnation point $\mathbf{r}_0$, has real coefficients and it is non-symmetric in the absence of molecular point-group symmetry. In the linear approximation,[37] only the first term in Eq.(2) is considered and the description of the field about a stagnation point amounts to solving three coupled linear differential equations arranged into a homogeneous system, where the matrix of the system is the Jacobian matrix. Reyn[38] reported a reference model of all possible phase portraits in the vicinity of a stagnation point and a classification in terms of the eigenvalues ξ_1, ξ_2, ξ_3 and eigenvectors $\mathbf{t}_1, \mathbf{t}_2, \mathbf{t}_3$ of the Jacobian matrix. A classification of stagnation points adopting the Euler index (*rank*, *signature*) has been proposed[18,19] and widely adopted.[2,7] The rank r is defined as the number of non-vanishing eigenvalues of the Jacobian matrix. The signature s is the excess of eigenvalues with a positive real part over a negative real part. The continuity equation $\nabla_\alpha J^{\mathbf{B}}_{\alpha} = 0$ implies that $\xi_1 + \xi_2 + \xi_3 = 0$, which poses a limit on the possible (r, s). Adopting a conventional nomenclature,[38] the allowed

cases are as follows.

- $(3, \pm 1)$ points corresponding to isolated singularities. The eigenvalues satisfy the condition $\xi_3 = -\Re(\xi_1 + \xi_2)$. If ξ_1 and ξ_2 are real then a node or a saddle is observed in the phase portrait of the flow over the plane of the eigenvectors $\mathbf{t}_1$ and $\mathbf{t}_2$. If ξ_1 and ξ_2 are complex conjugated, a focus is found.

- $(2, 0)$ points belong to stagnation lines, $\xi_3 = 0$ and $\xi_1 = -\xi_2$. If $\xi_{1,2}$ are real (pure imaginary) the phase portrait of a saddle (vortex) is observed. In the case of a saddle, the corresponding eigenvectors $\mathbf{t}_1$ and $\mathbf{t}_2$ are real and give the direction of the asymptotes through the singularity. In the case of a vortex, the two eigenvectors are complex. Saddle and vortex stagnation lines are continuous manifolds of $(2, 0)$ points. The eigenvector $\mathbf{t}_3$ is locally tangent to the stagnation line, which can be an open line, as in the case of an axial vortex, or form a close loop, as in the case of a toroidal vortex.

- $(0, 0)$ points correspond to transition singularities at which *branching* of stagnation lines may occur, $\xi_3 = \xi_1 = \xi_2 = 0$. From a mathematical point of view, these points correspond to a transition between pure imaginary and pure real eigenvalues.

The direction of flow about a singularity, a focus or vortex in particular, is determined by the vorticity, i.e., by the local curl $\left(\boldsymbol{\nabla} \times \mathbf{J}^{\mathbf{B}}\right)_{\mathbf{r}_0}$, which corresponds to the antisymmetric component of the Jacobian matrix.[2] Diamagnetic (paramagnetic) vortices of the electronic current density rotate clockwise (anti-clockwise) with respect to an observer placed at the north pole of the inducing magnetic field.

A very convenient way to search for singularities of $\mathbf{J}^{\mathbf{B}}(\mathbf{r})$ is a Newton-Raphson based procedure. Dropping out all non linear terms in the Taylor series expansion and setting the current density vector components to zero, one has (vector components by column)

$$\left[\mathbf{J}^{\mathbf{B}}\right]_{\mathbf{r}_2} \approx \left[\mathbf{J}^{\mathbf{B}}\right]_{\mathbf{r}_1} + \left[\boldsymbol{\nabla}\mathbf{J}^{\mathbf{B}}\right]_{\mathbf{r}_1} (\mathbf{r}_2 - \mathbf{r}_1) = \mathbf{0} \tag{3}$$

Accepted Version of J. Phys. Chem. A 2019, 123, 1558 doi: 10.1021/acs.jpca.8b10836

Then, choosing an arbitrary starting point $\mathbf{r}_1$, the following steps

$$1)\ \left[\boldsymbol{\nabla}\mathbf{J}^{\mathbf{B}}\right]_{\mathbf{r}_1}\mathbf{s} = -\left[\mathbf{J}^{\mathbf{B}}\right]_{\mathbf{r}_1}, \qquad 2)\ \mathbf{r}_2 = \mathbf{r}_1 + \mathbf{s}, \qquad 3)\ \mathbf{r}_1 = \mathbf{r}_2, \tag{4}$$

are repeated until the current density components are found less than a certain minimum criterion or a maximum number of steps has been taken. At the end of a successful search one has the Jacobian matrix, whose eigenvalues and eigenvectors permit to characterize the singularity as described above. The procedure is fast enough and the SG can be readily determined considering a sufficiently large number of starting points within the molecular region.

Stagnation graphs have revealed useful in a series of applications, such as the understanding of the proton magnetic shielding in benzene,[39] the study of the topology of the current density in diatropic monocyclic molecules,[40] the elaboration of the spatial ring current model of the [2.2]paracyclophane molecule,[41] the realization of topological models for the induced current density in small molecules,[42] the study of the induced paramagnetism and paratropism in closed-shell molecules,[43] the study of the magnetic-field induced electronic anapoles in small molecules.[44] Moreover, three-dimensional models of the quantum mechanical current density, induced in the electron cloud of the cyclopropane molecule by a uniform magnetic field applied either along the C_3 or the C_2 symmetry axes, have been constructed from the corresponding SGs.[34,45] These models of near Hartree-Fock quality have been used to interpret the exceptionally large in-plane component of the magnetic shielding in the centre of mass, which dominates the anomalous average of the tensor.

The SG of the current density induced by a magnetic field parallel to the main symmetry axis (i.e., perpendicular to the plane of the carbon atoms) calculated at the level of theory adopted in the present work, is given in Fig. 1. More figures and stereo-views of the SGs can be found in the Supporting Information. First of all, it is worth noting that these SGs well agree with previously reported ones obtained at the Hartree-Fock (HF) level using a

large basis set.[40,45] In particular, $(3, \pm 1)$ isolated singularities are predicted in same number and nearly same place: for benzene 24 saddle nodes and 12 foci on the molecular plane symmetrically placed aside carbon atoms; for cyclopropane 6 foci and 6 saddle nodes on the C-plane plus 12 out-of-plane foci.

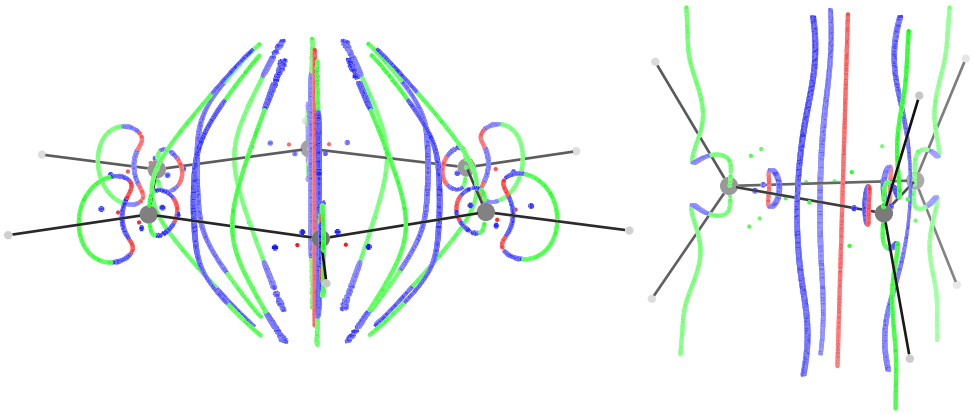

Figure 1: Stagnation graphs of the current density induced by a magnetic field perpendicular to the plane of the carbon atoms, for the benzene on the left and cyclopropane on the right. Colour code: blue is used to indicate isolated saddle nodes and saddle stagnation lines; red and green are used to indicate isolated foci and vortex stagnation line when $\mathbf{B} \cdot \left(\boldsymbol{\nabla} \times \mathbf{J}^{\mathbf{B}} \right)_{\mathbf{r}_0}$ is positive or negative, respectively. Accordingly the direction of the flow around a vortex line is paratropic or diatropic.

Molecular point group symmetry helps determine the overall features of the induced current density field and of its SG.[22] To discuss the symmetry of molecules in the presence of a magnetic field one has to consider magnetic groups.[46] Magnetic point groups $D_{6h}(C_{6h})$ and $D_{3h}(C_{3h})$ have to be used for benzene and cyclopropane, respectively. Then, according to the requirements posed by the magnetic symmetry, it can be observed that stagnation lines are entirely contained in $R\sigma$ planes (being R the time reversal operator) and that the symmetry axes C_n are necessarily stagnation lines, here paratropic vortex stagnation lines in both molecules.

The observed $(3, \pm 1)$ isolated singularities have a three-dimensional nature, as all of the eigenvalues of their Jacobian are nonzero. This introduces some difficulty, since, according to previous findings,[2,34] these singularities can be connected by a complex pattern of flow, which excludes the possibility of taking sums of purely rotational fields as previously noted.[47]

Accepted Version of J. Phys. Chem. A 2019, 123, 1558 doi: 10.1021/acs.jpca.8b10836

However, we remark that: i) far from isolated singularities the component of the current density parallel to the inducing magnetic field is usually small compared to the in-plane components; ii) as can be easily checked looking at Eqs.(5) and (6) for the magnetizability and magnetic shielding tensors, respectively,

$$\xi_{\alpha\delta} = \int \mathrm{d}V\, \Xi_{\alpha\delta}^{(\mathbf{r}_0)} = \frac{1}{2c}\epsilon_{\alpha\beta\gamma}\int \mathrm{d}V\ (r_\beta - r_{0\beta})\mathcal{J}_\gamma^{B_\delta}(\mathbf{r}), \tag{5}$$

$$\sigma_{\alpha\delta}^{I} = \int \mathrm{d}V\, \Sigma_{\alpha\delta} = -\frac{1}{c}\epsilon_{\alpha\beta\gamma}\int \mathrm{d}V\ \frac{r_\beta - R_{I\beta}}{|\mathbf{r}-\mathbf{R}_I|^3}\mathcal{J}_\gamma^{B_\delta}(\mathbf{r}), \tag{6}$$

for any given direction of observation, only the two perpendicular components of the current density are sufficient to determine the magnetic response. Incidentally, in eq. 5 and 6, we have introduced the magnetizability density and the nuclear magnetic shielding density,[48,49] that will be a matter of discussion in the following. The above observations have prompted us to exclude the component of the current density parallel to the inducing magnetic field and to introduce the pseudo-stagnation graph concept.[34] In the present case, the pseudo-SG can be obtained by formally setting $J_z^{\mathbf{B}} = 0$ and considering only the field over the xy plane, i. e., $\mathbf{J}_{xy}^{\mathbf{B}} = J_x^{\mathbf{B}}\mathbf{e}_1 + J_y^{\mathbf{B}}\mathbf{e}_2$. Although this suffices to determine the magnetic properties by means of Eqs.(5) and (6), we owe to recall that the two dimensional $\mathbf{J}_{xy}^{\mathbf{B}}$ has non-zero divergence due to the cancellation of the parallel component.

Pseudo-SGs corresponding to the SGs examined before are given in Fig.2. More figures and stereo-views of the pseudo-SGs can be found in the Supporting Information. An obvious observation is that all the stagnation lines and isolated singularities of one SG also belong to the corresponding pseudo-SG, which is eventually richer due to the cancellation of $J_z^{\mathbf{B}}$. As can be noted comparing Figs. 1 and 2, the isolated singularities of the SGs make part now of new closed stagnation lines, which are the only new entries in the pseudo-SGs. This confirms the same finding previously obtained at the HF level for cyclopropane[34] and extend the same consideration also to the benzene molecule. Looking carefully, it can be noticed that in cyclopropane the new closed stagnation lines are formed by one semi-portion that

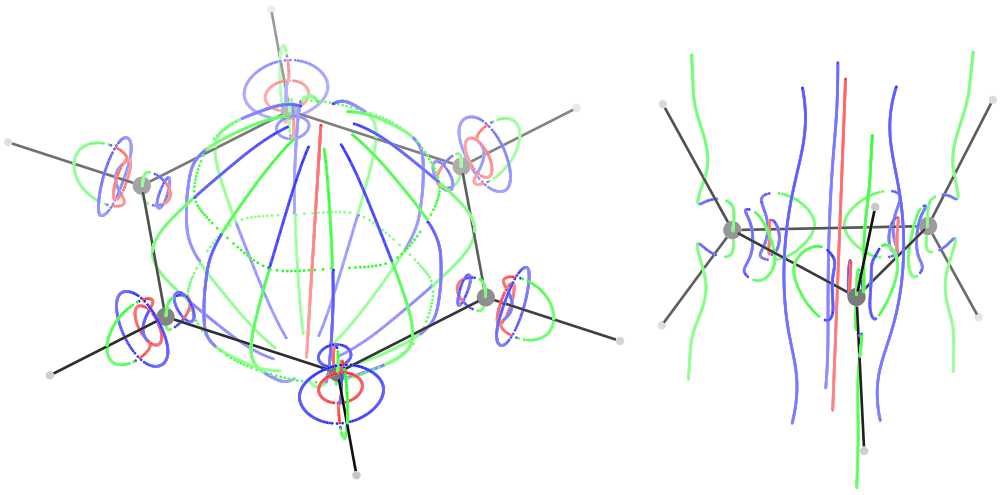

Figure 2: Pseudo-stagnation graphs of the current density induced by a magnetic field perpendicular to the plane of the carbon atoms, for the benzene on the left and cyclopropane on the right. See caption of Fig. 1 for further details.

is a saddle line and a second semi-portion that is a vortex line, whilst for benzene the new closed stagnation lines are entirely formed by a saddle line or a vortex line. In summary, 6 more mixed closed stagnation lines appear in the pseudo-SG of cyclopropane; 12 new closed saddle lines plus 6 new closed vortex line appear in the pseudo-SG of benzene.

3 Results and Discussion

3.1 Current density domains

Let us consider a $(2, 0)$ singular point belonging to a saddle line. As already mentioned, the non-zero eigenvalues ξ_1 and ξ_2 ($\xi_1 > \xi_2$) of its Jacobian matrix are real and opposite and the current density in its vicinity is two dimensional, flowing on the plane formed by the real eigenvectors $\mathbf{t}_1$ and $\mathbf{t}_2$. The essential feature of its portrait [7,38] is given by four boundary trajectories of the current density, whose asymptotes are given by the directions of the two eigenvectors.

Trajectories, or streamlines, of the current density vector field can be obtained by numerical solution of the real autonomous system of differential equations $\mathrm{d}\mathbf{r}/\mathrm{d}\tau = \mathbf{J}^{\mathbf{B}}(\mathbf{r})$, where

Accepted Version of J. Phys. Chem. A 2019, 123, 1558 doi: 10.1021/acs.jpca.8b10836

τ is some convenient coordinate along the trajectory.[7] Counting the trajectory, let say, in circular way, trajectories 1 and 3 (2 and 4) share the same asymptote. If the asymptote is given by the direction of $\mathbf{t}_1$ ($\mathbf{t}_2$), then the trajectories come out from (into) the saddle point. This implies the division of the plane in four *closed* sectors, since any other trajectory cannot came across the boundary lines.

When symmetry is present, as in the cases considered here, integrating the 4 boundary trajectories of a $(2,0)$ saddle node far enough they eventually match those emerging from symmetry related saddles, a behaviour found in a number of other examples.[47,50] This has been implemented taking the saddle points of a pseudo-SG and consistently integrating the boundary trajectories neglecting the component of the current density parallel to the inducing magnetic field. What is obtained corresponds to the superposition of long-range saddle phase portraits, which can be adequately termed a *saddle connection graph* (SCG).

Fig. 3 shows a selection of SCGs obtained for the benzene molecule on planes parallel to the molecular plane at various heights. The development of the current density field versus the distance from the C-plane can be appreciated at a glance: some compact toroidal vortices[7] having the diatropic centre on the carbon atoms disappear just over 0.2 bohr; more extended toroidal vortices having the diatropic centre close to the C-H bond middle persist up to 0.5 bohr; six diatropic vortices located on the C-C bonds remain present up to 1 bohr; then some branching occur up to a final branching point at about 2.5 bohr, where the central paratropic vortex dies down. A gap between the C-C bond vortices and the boundary streamlines that connect the C-H tori should be noted. Staking all together, something like a shape sand mould is obtained as shown in Fig. 4.

The interesting fact to note is that the current field is distinctly separated in a number of regions by the boundary trajectories, thus rendering the flow as a sum of separated islands of circulation. Exploiting the continuity of the saddle stagnation lines, the distance between the various SCGs can be reduced indefinitely, making the boundary trajectories on adjacent planes to melt together to form a surface, which can be referred to as a *separatrix*, after

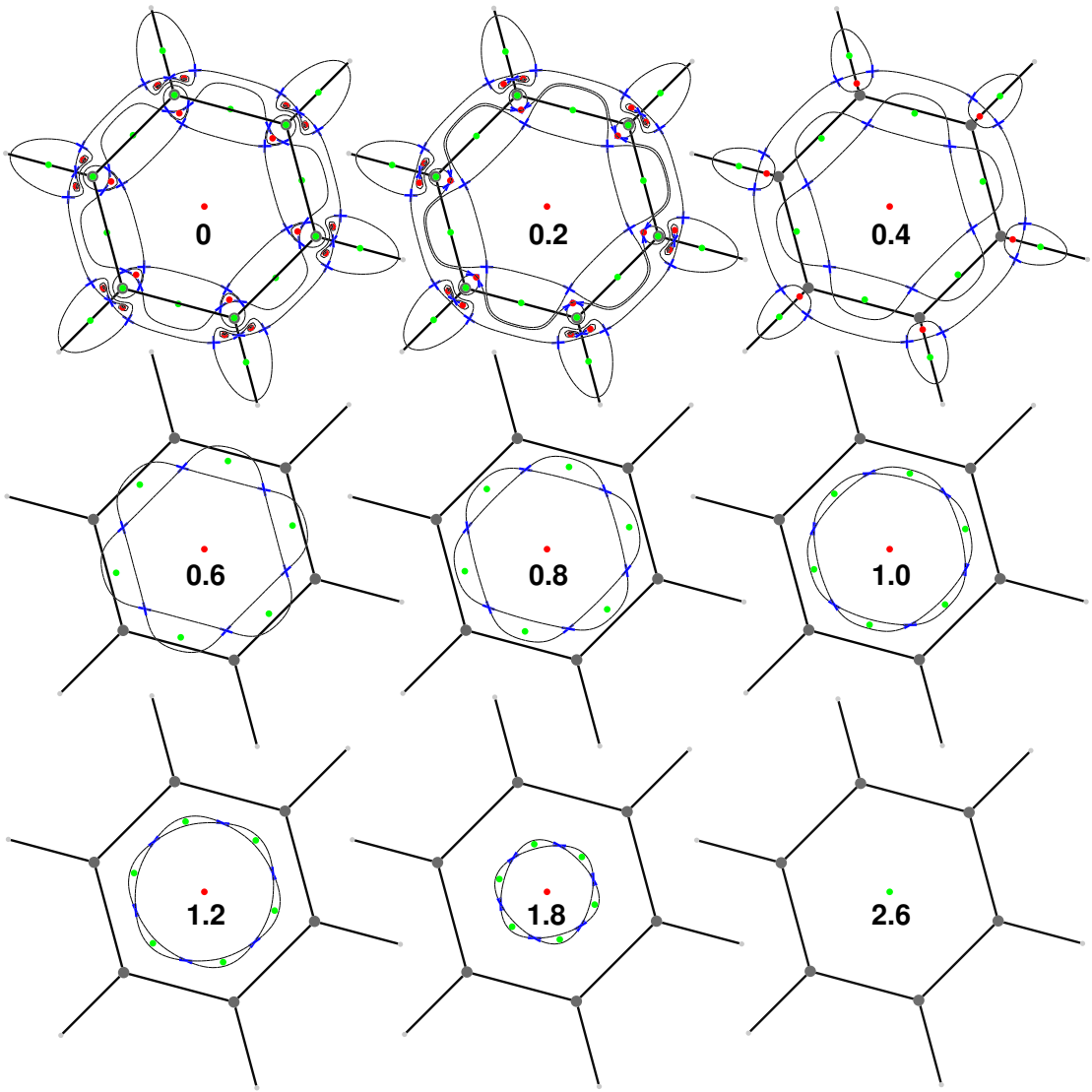

Figure 3: Saddle connection graphs (SCGs) of the benzene molecule. Saddle points, indicated by blue crosses, are from the pseudo-SG and boundary trajectories have been computed consistently assuming $J_z^{\mathbf{B}}$=0. Values indicate the distance in a.u. of the plotting plane from the symmetry σ_h plane. The external magnetic field is perpendicular and points toward the reader. Green (red) dots indicate diatropic (paratroopic) vortices.

Gomes.[19] The term separatrix is rather meaningful, since it makes a great analogy with a container that encloses the flow of current in its interior: whichever trajectory of the current cannot perforate a separatrix. Therefore, each molecular region inside a separatrix constitutes a *domain* of the current density. The term domain is strictly connected with that of integration domain, see hereafter the discussion on the decomposition of magnetic

The Journal of Physical Chemistry
Accepted Version of J. Phys. Chem. A 2019, 123, 1558 doi: 10.1021/acs.jpca.8b10836

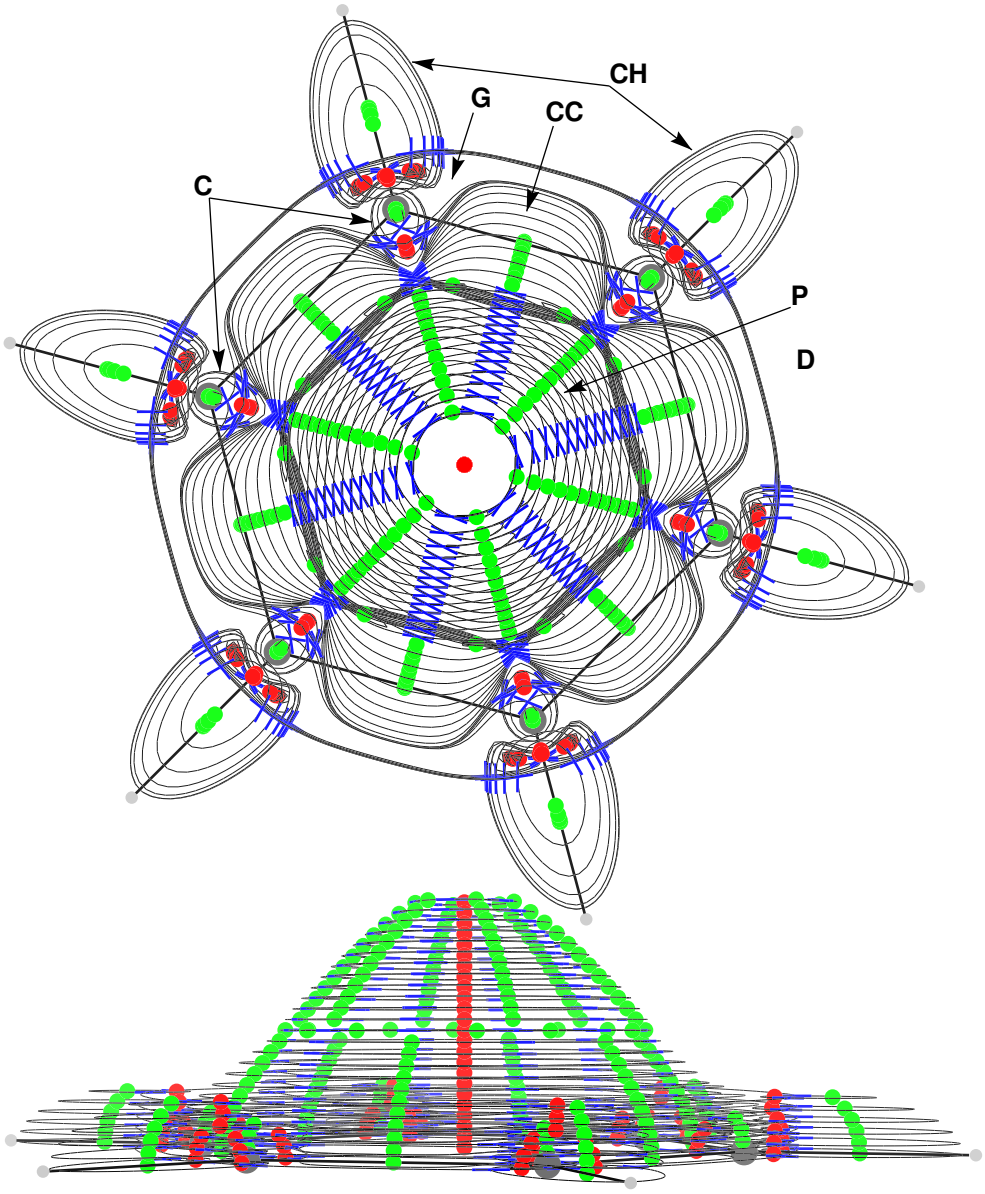

Figure 4: Top and side views of the SCG stack of the benzene molecule. Letters indicate the domains of the current density. Only the upper half is represented, an equivalent part is on the other side of the σ_h symmetry plane.

properties.

In Fig. 4 the current density domains of the benzene molecule have been indicated by a label in the following way: domains **C**, enclosing local circulations around carbon atoms; domains **CH**, enclosing local circulations around C-H bonds; domains **CC**, enclosing local circulations around C-C bonds; an extended domain **P** of paratropic current enveloping

the main symmetry axis; a delocalized domain **G** delimited by domains **C**, **CC** and **CH**, enclosing a diatropic flow of current. All the above domains are immersed within a unique large domain of diatropic current indicated with the letter **D**, which drops down as the electron charge distribution goes to zero in the tail molecular region.

As it concerns the cyclopropane molecule, the same procedure applied to the benzene molecule has produce the selection of SCGs shown in Fig. 5 for a perpendicular inducing magnetic field.

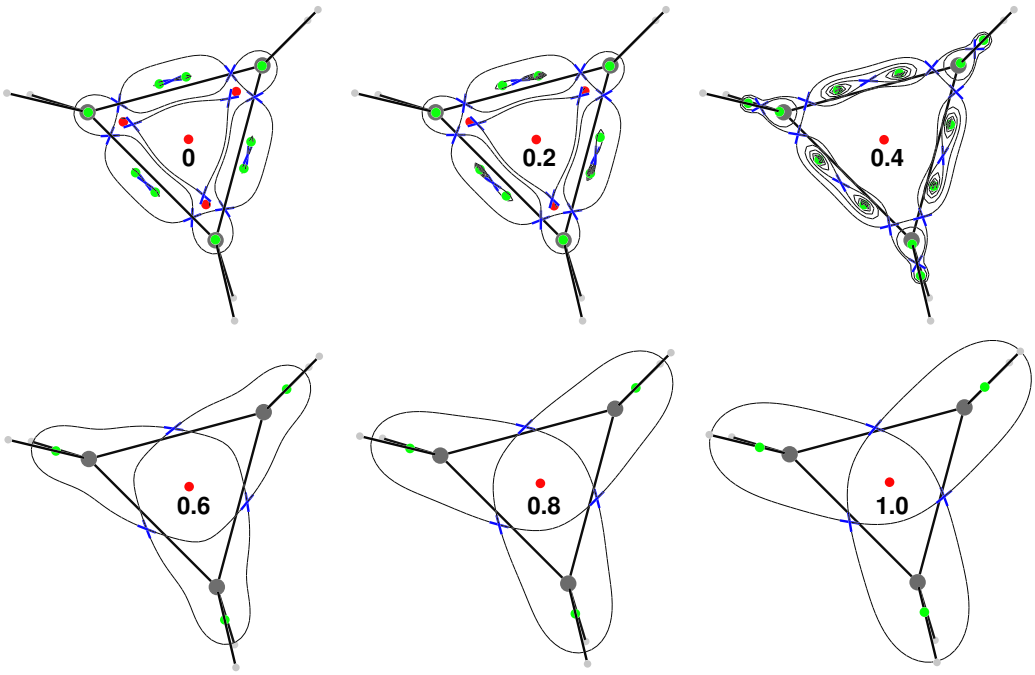

Figure 5: Saddle connection graphs (SCGs) of the cyclopropane molecule. See caption of Fig. 3 for further details.

The development of the current density flow varying the distance from the plane of the carbon atoms shows the relevant domains of the cyclopropane current density, which have been labelled as indicated in Fig. 6. Although significantly different respect to the benzene molecule, maps show some common features, such as: domains **C** and **CC**, enclosing diatropic local circulations around carbon atoms and C-C bonds, respectively; an extended domain **P** of paratropic current enveloping the main symmetry axis. Along the C-H bond regions the boundary streamlines form a kind of three-rim stem glass, which is formed by

The Journal of Physical Chemistry
Accepted Version of J. Phys. Chem. A 2019, 123, 1558 doi: 10.1021/acs.jpca.8b10836

the union of three domains **CH** of diatropic current enclosing the central paratropic domain. All around, a unique large domain of diatropic current dropping down as ρ goes to zero, indicated with the letter **D**, encloses everything.

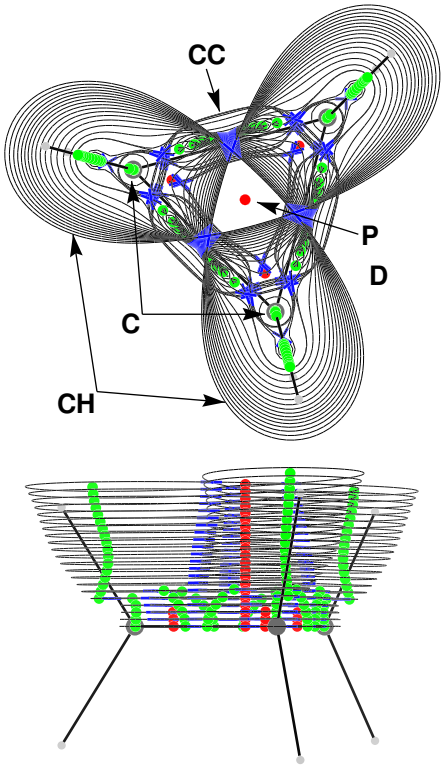

Figure 6: Top and side views of the SCG stack of the cyclopropane molecule. Letters indicate the domains of the current density. Only the upper half is represented, an equivalent part is on the other side of the σ_h symmetry plane.

At this point, one might wonder whether the inclusion of $J_z^{\mathbf{B}}$ could produce a different picture. To this purpose, we have calculated the SCGs integrating the boundary trajectories using the three-dimensional current density field. The resulting SCG stacks are given in the supporting information. As it can be observed, the confinement of the flow is pretty the same; streamlines present only a small deviation from planarity. In benzene the major difference is given by some small spirals in proximity of the branching points delimiting the upper part of domains **CC**; in cyclopropane some difference is discernible in the region delimiting **C** and domains **CH**. Since the most relevant features of the current density flow have been grasped by the two-dimensional integration of the boundary trajectories and allowing for a

lesser degree of difficulty, we decided to carry on this way for the detachment of the current density domains and for the molecular magnetic property decomposition described hereafter.

3.2 Current density domain separation

In this section the procedure developed to take apart the various current density domains is described. This is a required step to prove what stated before and to collect the separatrices for the partition of the magnetic properties.

Let us consider first the most simple case formed by a unique saddle stagnation line between two vortex stagnation lines having the same tropicity. For example, this is the case of hydrogen bonded systems, for which the decomposition of the proton magnetic shielding in terms of current density domain contributions has permitted to rationalize the large down-field shift of the proton magnetic resonance that is considered one of the best evidences for hydrogen bond formation.[51] The two domains attached to this single saddle stagnation line can be conveniently taken apart in the following way. For each saddle node, we take into account the eigenvector $\mathbf{t}_1$ associated with the positive eigenvalue ξ_1 of its Jacobian matrix; $\mathbf{t}_1$ provides the direction of the two boundary trajectories coming out from the saddle. Both trajectories close on the same saddle node approaching the asymptote described by $\mathbf{t}_2$. Therefore, integrating the boundary trajectories one at a time, and repeating the calculation for each saddle node along the stagnation line, it is easy to devise a way to collect separately the streamlines that form the two separatrices.

In a more general case, one has also to consider that boundary trajectories starting from one saddle line could end on a different one, in more than one way, and that many saddle lines should be used to form the same separatrix. This complex information is provided by the SCGs. For each SCG an algorithm has been adapted from a recently developed method for the search of the smallest set of smallest rings (SSSR),[52] which provides all the circuits connecting the saddle nodes. With respect to the SSSR, our algorithm exploits also the versus of each connection, which helps greatly to accomplish the task. Then, looping on the

The Journal of Physical Chemistry
Accepted Version of J. Phys. Chem. A 2019, 123, 1558 doi: 10.1021/acs.jpca.8b10836

SCG stack, the procedure sorts the detected circuits into different separatrices on the basis of a similarity criterion, i.e., all the circuits forming a separatrix must connect the same number of saddle nodes belonging to the same saddle stagnation lines. Eventually, a final selection removes all those separatrices that are too small to be useful.

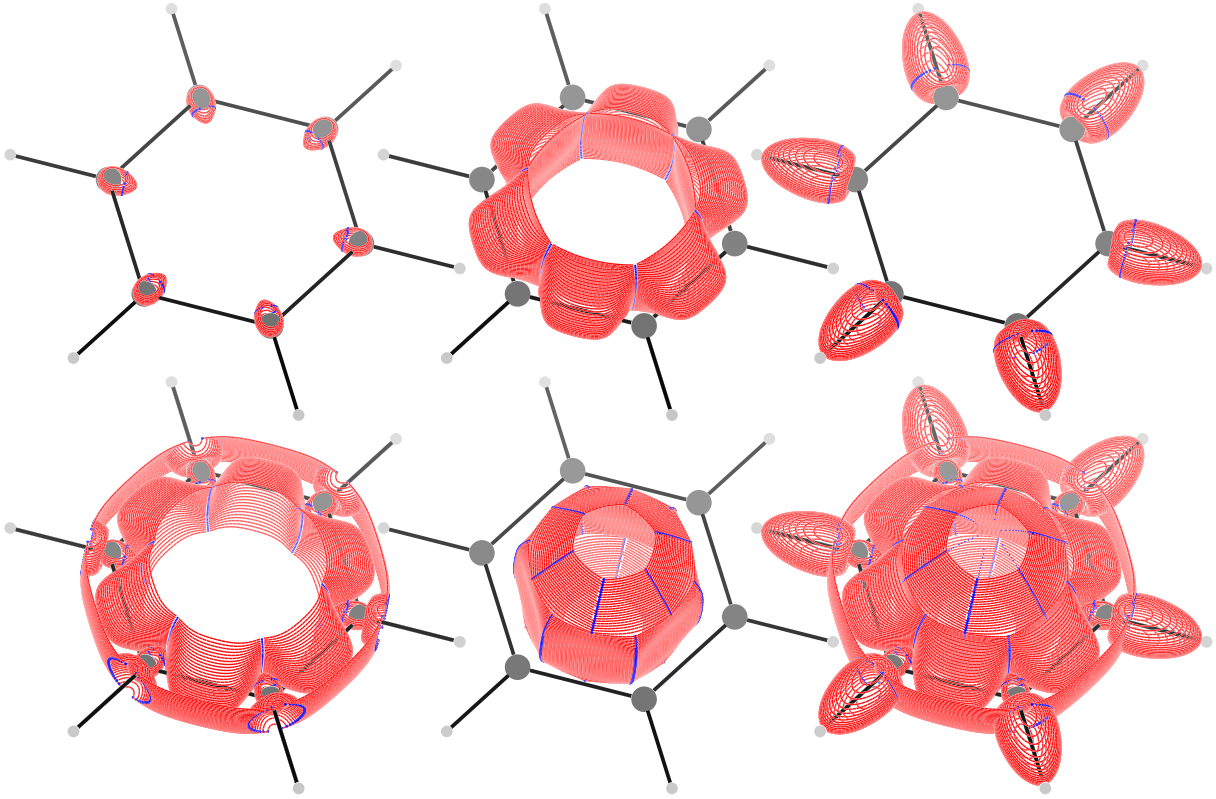

Figure 7: Domains of the current density induced by a magnetic field parallel to the main symmetry axis of the benzene molecule. Top row, from left to right: domain **C**, **CC**, and **CH**. Bottom row, from left to right: domain **G**, **P**, and assembled domains.

The procedure applied to the benzene molecule has produced the result shown in Fig. 7. The boundary trajectories forming each separatrix are plotted in red. Small blue dots mark the position of the saddle nodes used to compute the connecting circuits. The current density domains perceived by inspection of Fig. 4 are now taken apart and enclosed in their own separatrix. As a check of the goodness of the result, the five benzene current density domains are then assembled together again, into some sort of a 3D molecular puzzle, to obtain the last plot in Fig. 7, which reproduces nicely the SCG stack of Fig. 4. In summary 5 different

current density domains have been separated corresponding to those described previously. Interesting enough is the isolation of the domain **G** that, owing to its disposition close to the plane of the carbon atoms and its extension, indicates the presence of a diatropic σ-electron ring current, in addition to the inner paratropic σ-electron ring current inside domain **P**. Actually, one should not forget that these five domains contain only a fraction of the total current density field, the remaining current flows inside the most external domain **D** of delocalized diatropic current, which encloses everything dropping down in the tail molecular region. In order to better view the arguments exposed so far, an animation has been included within the supporting information that shows the flow confined within domain **P**. The animation permits also to grasp the confinement of the current density within the other domains.

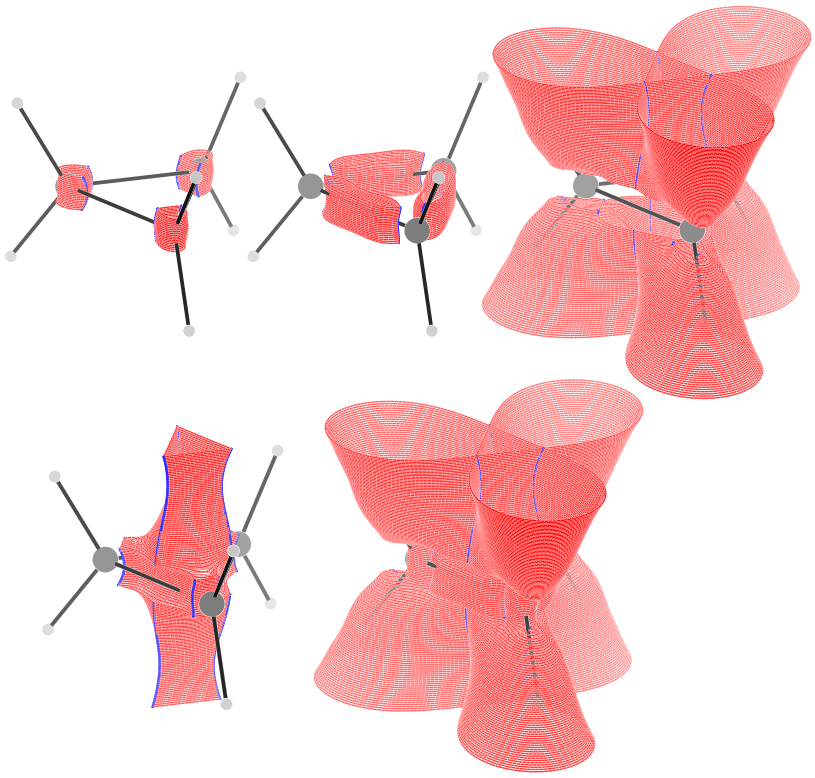

Figure 8: Domains of the current density induced by a magnetic field parallel to the main symmetry axis of the cyclopropane molecule. Top row, from left to right: domain **C**, **CC**, and **CH**. Bottom row, from left to right: domain **P**, and assembled domains.

Accepted Version of J. Phys. Chem. A 2019, 123, 1558 doi: 10.1021/acs.jpca.8b10836

For the cyclopropane molecule the current density domains perceived by inspection of Fig. 6 are shown taken apart in Fig. 8. The plotting conventions are the same as in benzene. With respect to the latter, it is interesting to note slightly more extended current domains around the carbon atoms and sensibly more compact current domains for the C-C bond region. The domain **P** containing the central paratropic flow is rather extended near the σ_h symmetry plane and is compressed by the diatropic domains **CH** in conjunction with the closing of the domains **C** and **CC**. It is quite interesting to note the narrowing around the carbon atom plane, where the external domain **D** squeezes the local flows. In this region is where the diatropic σ-electron ring current occurs. A plot showing the superposition of the σ-electron ring current with the local domains is given within the supporting information.

In both molecules, the current density within each inner and external domains contribute differently to the total out-of-plane component of the molecular magnetic properties. This is examined in the next section.

3.3 Breakdown of the molecular magnetic properties into domain contributions

The partition of the molecular space through the separatrices of the current density as shown above is fundamentally different from that provided by the QTAIM, which permits current flow out of the atomic basins.[3] To better appreciate this point, we shall consider in the following the partitions of the magnetizability ξ_{zz} and of the nuclear magnetic shielding, σ^I_{zz}, which are integral properties of the corresponding densities as defined in eqs. (5) and (6). As the shielding density is origin-independent, any partition of the molecular space in subspaces $\mathcal{D}$ will end up in a partition of the molecular property,

$$\sigma^I_{zz} = \sum_{\mathcal{D}} \sigma^I_{zz,\mathcal{D}}, \tag{7}$$

where each contribution $\sigma^I_{zz,\mathcal{D}}$ is origin-independent. This is not the case for the magnetizability, where one has

$$\xi_{zz} = \sum_{\mathcal{D}} \xi_{zz,\mathcal{D}}, \tag{8}$$

and the contributions $\xi_{zz,\mathcal{D}}$ generally do depend on the origin, as could be expected from inspection of eq.(5). Indeed, for two independently chosen origins $\mathbf{r}_0$ and $\mathbf{r}'_0$, such that $\mathbf{r}'_0 = \mathbf{r}_0 + \mathbf{d}$, assuming $\mathbf{B} = \mathbf{k}B_z$, one has

$$\begin{aligned}
\xi'_{zz,\mathcal{D}} &= \frac{1}{2}\epsilon_{z\beta\gamma}\int_{\mathcal{D}}(r_\beta - r'_{0\beta})\mathcal{J}^{B_z}_\gamma d\mathcal{D} = \\
&= \frac{1}{2}\epsilon_{z\beta\gamma}\left[\int_{\mathcal{D}}(r_\beta - r_{0\beta})\mathcal{J}^{B_z}_\gamma d\mathcal{D} - d_\beta\int_{\mathcal{D}}\mathcal{J}^{B_z}_\gamma d\mathcal{D}\right] = \\
&= \xi_{zz,\mathcal{D}} - \frac{1}{2}\epsilon_{z\beta\gamma}d_\beta\int_{\mathcal{D}}\mathcal{J}^{B_z}_\gamma d\mathcal{D}.
\end{aligned} \tag{9}$$

Thus, in order to have origin-independent contributions, the integral in the last term of eq.(9) should vanish. That condition can be recast as follows. Let us consider the equality

$$\boldsymbol{\nabla}\cdot\left(\mathbf{J}^{\mathbf{B}}f\right) = f\boldsymbol{\nabla}\cdot\mathbf{J}^{\mathbf{B}} + \mathbf{J}^{\mathbf{B}}\cdot\boldsymbol{\nabla}f, \qquad \forall\mathbf{r}, \tag{10}$$

where, for the sake of space, $\mathbf{J}^{\mathbf{B}} = \mathbf{J}^{\mathbf{B}}(\mathbf{r})$ and $f = f(\mathbf{r})$ is any arbitrary scalar function. Owing to the continuity condition for stationary states, $\boldsymbol{\nabla}\cdot\mathbf{J}^{\mathbf{B}} = 0$, eq.(10) reduces to

$$\boldsymbol{\nabla}\cdot\left(\mathbf{J}^{\mathbf{B}}f\right) = \mathbf{J}^{\mathbf{B}}\cdot\boldsymbol{\nabla}f, \qquad \forall\mathbf{r}. \tag{11}$$

Integrating both sides of the above equation over the subspace $\mathcal{D}$, one has

$$\int_{\mathcal{D}}\boldsymbol{\nabla}\cdot\left(\mathbf{J}^{\mathbf{B}}f\right)d\mathcal{D} = \int_{\mathcal{D}}\mathbf{J}^{\mathbf{B}}\cdot\boldsymbol{\nabla}f\,d\mathcal{D}. \tag{12}$$

Accepted Version of J. Phys. Chem. A 2019, 123, 1558 doi: 10.1021/acs.jpca.8b10836

According to the divergence theorem, the volume integral on the left hand side of the above equation can be converted into a surface integral over the boundary of volume $\mathcal{D}$. Therefore,

$$\int_{\mathcal{D}} \mathbf{J}^{\mathbf{B}} \cdot \boldsymbol{\nabla} f d\mathcal{D} = \oint_{\mathcal{S}} f \mathbf{J}^{\mathbf{B}} \cdot \mathbf{n} d\mathcal{S}, \tag{13}$$

where $\mathbf{n}$ is the outward pointing unit vector perpendicular to the infinitesimal surface element $d\mathcal{S}$. In particular, setting the arbitrary function $f = r_\gamma$, one has that the integral in the last term of eq.(9) becomes

$$\int_{\mathcal{D}} \mathcal{J}_\gamma^{\mathbf{B}} d\mathcal{D} = \oint_{\mathcal{S}} r_\gamma \mathbf{J}^{\mathbf{B}} \cdot \mathbf{n} d\mathcal{S}. \tag{14}$$

Therefore, specializing for our initial choice $\mathbf{B} = \mathbf{k}B_z$, if there is current crossing the boundary of the domain, the component $\xi_{zz,\mathcal{D}}$ will be origin-dependent. Bader and Keith devised an elegant way out of the problem, adding and subtracting an origin-dependent contribution for each surface separating a pair of subspaces.[3] This recipe depends however both on the space partition chosen, e.g. QTAIM basins, Voronoi cells[53] or whatever other partition, and on the point chosen on the surface separating each pair of subspaces.

These limitations are absent for the method introduced in the present paper. Starting from the most general case of a separatrix formed by the union of boundary trajectories obtained integrating the 3-dimensional current density field, one would arrive at something like an impenetrable wall that prevents the passage of current between domains, i.e., the flux in the current density over such a separatrix would be vanishing at any point, as given by

$$\mathbf{J}^{\mathbf{B}}(\mathbf{r}) \cdot \mathbf{n}(\mathbf{r}) = 0, \qquad \forall \mathbf{r} \in \mathcal{S}, \tag{15}$$

where $\mathbf{n}(\mathbf{r})$ is a unit vector normal to the separatrix at $\mathbf{r}$. In this case, eq.(14), together with $\mathbf{B} = \mathbf{k}B_z$, becomes

$$\int_{\mathcal{D}} \mathcal{J}_\gamma^{B_z} d\mathcal{D} = 0. \tag{16}$$

The above equation, when inserted in eq.(9), shows that the magnetizability contributions

$\xi_{zz,\mathcal{D}}$ are origin-independent. Incidentally, eq. (16) shows that the integral condition for the charge current conservation over the full molecular space[54,55] holds also for each closed domain of the current density.

In the present approach, separatrices have been obtained integrating the components of the current density perpendicular to the inducing magnetic field. Therefore, eq.(15) does not hold and in its place we have the modified condition

$$\mathbf{J}^{\mathbf{B}}_{\perp}(\mathbf{r}) \cdot \mathbf{n}(\mathbf{r}) = 0, \qquad \forall \mathbf{r} \in \mathcal{S}, \tag{17}$$

where $\mathbf{J}^{\mathbf{B}}_{\perp} = \mathbf{J}^{\mathbf{B}} - J^{\mathbf{B}}_{z}\mathbf{k}$. Then, substituting $\mathbf{J}^{\mathbf{B}} = \mathbf{J}^{\mathbf{B}}_{\perp} + J^{\mathbf{B}}_{z}\mathbf{k}$ in eq.(14) and using eq.(17) one has

$$\int_{\mathcal{D}} \mathcal{J}^{\mathbf{B}}_{\gamma} d\mathcal{D} = \oint_{\mathcal{S}} r_{\gamma} J^{\mathbf{B}}_{z} \mathbf{k} \cdot \mathbf{n} d\mathcal{S}. \tag{18}$$

In general $\mathbf{n}$ is not perpendicular to $\mathbf{k}$ and the *integrand* on the rhs of the above equation is not vanishing, although it can be expected to be small due to the presence of the typically negligible non classical component of the current density, $J^{B_z}_{z}$ in our case. At any rate, the *integral* could still be vanishing as we will discuss later on.

In practical calculations, performed using basis sets containing a finite number of basis functions, the continuity equation $\nabla_{\alpha} J^{\mathbf{B}}_{\alpha}$ is not vanishing and equation (11) and all that follows is not exactly fulfilled. However, using basis sets of adequate size containing several polarization functions, the current density leakage problem can be substantially reduced.

All the above demonstrates the possibility to decompose the magnetic properties in a rather natural way exploiting the topology of the induced current density field and offers a different point of view from that given by Bader and Keith with their method of the properties of atoms in molecules.[3]

Accepted Version of J. Phys. Chem. A 2019, 123, 1558 doi: 10.1021/acs.jpca.8b10836

3.4 Numerical results

The breakdown into current density domain contributions of the out-of-plane component of the molecular magnetic properties of the benzene molecule is shown in Table 1. Looking at the reported values, some of them appear very comprehensible, whilst other permit to see something never reported before. The out-of-plane component of the carbon magnetic shielding shows perhaps the less surprising decomposition. In fact, the major contribution comes from one of the six very small domains **C**, i. e., that containing the carbon nucleus in question, where the current density is very large, in agreement with the $1/r^2$ factor of the shielding density function. Nevertheless, almost 44 ppm, nearly 25% of the total component, come from the two domains of delocalized flow **D** and **G**. Of course, only the flow fractions closer to the nucleus give these substantial contributions. Contributions to σ_{zz}^{C} from domains **P**, **CC**, and **CH**, are not very significant. The small shielding/de-shielding effect from domain **CC**/**P** should be noted.

Table 1: Decomposition of the out-of-plane component of the magnetic shieldings and magnetizability tensors of the benzene molecule into current density domain contributions (magnetic shielding in ppm, magnetizability in 10^{-30} J T^{-2})

Prop.	**P**	**CC**	**C**	**CH**	**G**	**D**	Tot	Expt
σ_{zz}^{C}	1.8	-2.0	135.4	0.1	10.4	33.5	179.1	
σ_{zz}^{H}	0.3	-0.1	0.0	-1.4	-0.9	23.2	21.0	
$\sigma_{zz}^{\mathrm{CM}}$	-27.8	-2.1	0.0	0.0	5.8	40.4	16.2	
ξ_{zz}	42.9	-7.2	-2.7	-8.3	-88.1	-1570.0	-1633.3	-1570±42[56]

As can be observed in Figs. 4 and 7, hydrogen nuclei are immersed within the domain **D**, just outside the domains **CH**. As a consequence of this disposition and of the $1/r^2$ factor, σ_{zz}^{H} is almost completely determined by the current density inside the domain **D** in the vicinity of the nucleus. A bit surprising is the small contribution form the closer domain **CH**. A de-shielding effect as large as 1 ppm from **G** should be noted.

The breakdown of $\sigma_{zz}^{\mathrm{CM}}$ deserves a special consideration, since the negative of this quantity is used to define the out-of-plane component of the nucleus independent chemical shift

(NICS$_{zz}$) tensor, introduced as a better index of the aromatic character of electronic π system[57] with respect to the very well known isotropic NICS.[58] Its breakdown clearly shows how much NICS$_{zz}$ is still contaminated by σ-electron contributions coming from: i) the domain **P** that largely de-shields (nearly -28 ppm) the centre of mass; ii) the domain **G** that gives a fairly large shield of about 6 ppm. A more realistic value of the π-electron shielding effect on the centre of mass can be accounted by the contribution coming from the domain **D**, even if domain separation is not the same as σ/π-electron separation. Then, taking the **D** contribution, we surely overestimate the magnitude of the benzene NICS$_{\pi zz}$ to -40.4 ppm, to be compared with -36.15 ppm obtained at the B3LYP/6-31+G* level by Fallah-Bagher-Shaidaei et al.[59]

As far as it concerns the decomposition of the out-of-plane magnetizability, it should be appreciated that the integral on the rhs of eq.(18) is exactly vanishing by symmetry. This happens because each current density domain is crossed by a σ_h symmetry plane of the magnetic point groups $D_{6h}(C_{6h})$,[46] which separates the integral in two equal and opposite parts. As a consequence each magnetizability contribution is origin independent. The decomposition of the benzene ξ_{zz} shows that localized contributions coming from domains **CC**, **C**, and **CH** are negligible compared to those given by delocalized domains **P**, **G**, and **D**. The results are comprehensible on the basis that the delocalized circulations span a much larger area with respect to the localized ones. Perhaps, a bit surprising is the extent of the difference between the two kind of circulation: localized contributions can be safely not counted at all, for the benzene molecule at least. Among the delocalized contributions, that coming from the domain **D** is dominating, i. e., the role of the diatropic π-electron ring current is fundamental in this case.

The breakdown into current density domain contributions of the out-of-plane component of the molecular magnetic properties of the cyclopropane molecule is shown in Table 2. Also in this case, domain **D** gives a large contribution that is dominant, except in σ^{C}_{zz}. It should be noted that in cyclopropane the domain **D** contains a diatropic σ-electron delocalized

Accepted Version of J. Phys. Chem. A 2019, 123, 1558 doi: 10.1021/acs.jpca.8b10836

Table 2: Decomposition of the out-of-plane component of the magnetic shieldings and magnetizability tensors of the cyclopropane molecule into current density domain contributions (magnetic shielding in ppm, magnetizability in 10^{-30} J T^{-2})

Prop.	**P**	**CC**	**C**	**CH**	**D**	Tot	Expt
σ_{zz}^{C}	0.3	-0.2	158.9	4.6	62.2	225.8	
σ_{zz}^{H}	0.0	0.0	0.0	12.1	23.9	36.1	
σ_{zz}^{CM}	-13.1	-0.3	-0.2	0.6	45.0	32.0	
ξ_{zz}	2.6	-1.1	-2.1	-55.8	-744.0	-800.3	-779±18 [60]

flow, which can be recognized as a σ-electron ring current on the plane of the carbon atoms. Therefore, cyclopropane is often referred to show σ-aromaticity on the magnetic criterion. However, great care should be used assuming such a definition, especially adopting the NICS as an aromaticity indicator, since, as it has been clearly shown,[34,45] the big average virtual shielding evaluated at the centre of mass is mainly determined by an exceptionally large in-plane component of nearly 50 ppm, to be compared with the out-of-plane component of 32 ppm.

Beside the contribution coming from domain **D**, the out-of-plane component of each property obtains another large contribution form a second domain, namely: σ_{zz}^{C} from domain **C** (58.9 ppm, 70% of the total); σ_{zz}^{H} from domain **CH** (12.1 ppm, roughly 1/3 of the total); σ_{zz}^{CM} from domain **P** (-13 ppm, roughly 40% of the total, but with opposite sign); and ξ_{zz} from domain **CH**, contributing by only 7% of the total. Contributions coming from other domains are negligible.

4 Conclusions

A partition scheme of the current density induced at first-order by a magnetic field perpendicular to the plane of carbon atoms of the benzene and cyclopropane molecules has been presented. The scheme is obtained by subjecting the current density field to a topological analysis, which provides current domains delimited by separatrices formed by the union of

all the current trajectories connecting saddle lines of the pseudo-stagnation graph. These domains give a faithful representation of the current regime in terms of local vortices embedded into a delocalized flow of current, in a way that reminds the inclusion of matryoshka dolls one inside another. As a consequence, a breakdown of the parallel component of the magnetic shielding and magnetizability into origin independent domain contributions has been obtained.

We found that, for the parallel component of magnetizability and magnetic shielding at ^{13}C, ^{1}H, and centre of mass, a large contribution derives from the current density delocalized all over the molecules. Such a contribution is unexpectedly large even in the case of benzene and cyclopropane, which are archetypal of $\pi-$ and $\sigma-$aromaticity. In the case of the magnetizability, the ratio of localized to delocalized contributions amounts to 1% and 8% for benzene, and cyclopropane, respectively.

It is interesting to compare these ratios with the corresponding ones obtained by the atomic partition of Bader and Keith (BK), i.e., the ratios of basin and surface contributions, which are 38% and 124% for benzene and cyclopropane, respectively. This qualitative disagreement can be understood because the basin contributions by BK are heavily affected by delocalized currents, as can be appreciated by direct inspection of the current density maps, both those reported here, and those reported by BK.[3]

Acknowledgement

The authors thanks the "Ministero Italiano per l'Università e la Ricerca", FARB 2016, for financial support.

Supporting Information Available

The following files are available free of charge.

Accepted Version of J. Phys. Chem. A 2019, 123, 1558 doi: 10.1021/acs.jpca.8b10836

- Sup_Inf.pdf: stereo views of SGs and pseudo-SGs; top and side views of SGs and pseudo-SGs; separatrices obtained integrating trajectories from the three-dimensional current density field; animation of the current flow superimposed to the innermost paratropic domain in benzene; superposition of separatrices and current density field in cyclopropane.

This material is available free of charge via the Internet at `http://pubs.acs.org/`.

References

(1) Keith, T. A.; Bader, R. F. Calculation of Magnetic Response Properties Using a Continuous Set of Gauge Transformations. *Chem. Phys. Lett.* **1993**, *210*, 223–231.

(2) Keith, T. A.; Bader, R. F. W. Topological Analysis of Magnetically Induced Molecular Current Distributions. *J. Chem. Phys.* **1993**, *99*, 3669–3682.

(3) Bader, R. F. W.; Keith, T. A. Properties of Atoms in Molecules: Magnetic Susceptibilities. *J. Chem. Phys.* **1993**, *99*, 3683–3693.

(4) Lazzeretti, P.; Malagoli, M.; Zanasi, R. Computational Approach to Molecular Magnetic Properties by Continuous Transformation of the Origin of the Current Density. *Chem. Phys. Lett.* **1994**, *220*, 299–304.

(5) Steiner, E.; Fowler, P. W. Four- and Two-electron Rules for Diatropic and Paratropic Ring Currents in Monocyclic π Systems. *Chem. Commun.* **2001**, 2220–2221.

(6) Steiner, E.; Fowler, P. W. Patterns of Ring Currents in Conjugated Molecules: A Few-Electron Model Based on Orbital Contributions. *J. Phys. Chem. A* **2001**, *105*, 9553–9562.

(7) Lazzeretti, P. Ring Currents. *Prog. Nucl. Magn. Reson. Spectrosc.* **2000**, *36*, 1–88.

(8) Fowler, P. W.; Steiner, E.; Havenith, R. W. A.; Jenneskens, L. W. Current Density, Chemical Shifts and Aromaticity. *Magn. Reson. Chem.* **2004**, *42*, S68–S78.

(9) Coriani, S.; Lazzeretti, P.; Malagoli, M.; Zanasi, R. On CHF Calculations of Second-order Magnetic Properties Using the Method of Continuous Transformation of Origin of the Current Density. *Theor. Chim. Acta* **1994**, *89*, 181–192.

(10) London, F. Théorie Quantique du Diamagnetism des Combinaisons Aromatiques. *Comptes Rendus Acad. Sci.* **1937**, *205*, 28–30.

(11) London, F. Théorie Quantique des Courants Interatomiques dans les Combinaisons Aromatiques. *J. Phys. Radium* **1937**, *8*, 397–409.

(12) Cheeseman, J. R.; Trucks, G. W.; Keith, T. A.; Frisch, M. J. A Comparison of Models for Calculating Nuclear Magnetic Resonance Shielding Tensors. *J. Chem. Phys.* **1996**, *104*, 5497–5509.

(13) Sundholm, D.; Fliegl, H.; Berger, R. J. Calculations of Magnetically Induced Current Densities: Theory and Applications: Calculations of Magnetically Induced Current Densities. *WIREs Comput. Mol. Sci.* **2016**, *6*, 639–678.

(14) Becke, A. D. A Multicenter Numerical Integration Scheme for Polyatomic Molecules. *J. Chem. Phys.* **1988**, *88*, 2547–2553.

(15) Lazzeretti, P.; Zanasi, R. Inconsistency of the Ring-current Model for the Cyclopropenyl cation. *Chem. Phys. Lett.* **1981**, *80*, 533–536.

(16) Lazzeretti, P.; Rossi, E.; Zanasi, R. Theoretical Studies on the Benzene Molecule. II. Criticism of the Ring Current Model. *J. Chem. Phys.* **1982**, *77*, 3129–3139.

(17) Lazzeretti, P.; Rossi, E.; Zanasi, R. Nuclear Magnetic Shielding in Cyclopropane and Cyclopropenyl Cation. *J. Am. Chem. Soc.* **1983**, *105*, 12–15.

Accepted Version of J. Phys. Chem. A 2019, 123, 1558 doi: 10.1021/acs.jpca.8b10836

(18) Gomes, J. A. N. F. Topological Elements of the Magnetically Induced Orbital Current Densities. *J. Chem. Phys.* **1983**, *78*, 4585–4591.

(19) Gomes, J. A. N. F. Topology of the Electronic Current Density in Molecules. *Phys. Rev. A* **1983**, *28*, 559–566.

(20) Lazzeretti, P.; Rossi, E.; Zanasi, R. Singularities of Magnetic-field Induced Electron Current Density: A Study of the Ethylene Molecule. *Int. J. Quantum Chem.* **1984**, *25*, 929–940.

(21) Lazzeretti, P.; Rossi, E.; Zanasi, R. Magnetic Properties and Induced Current Density in Acetylene. *Int. J. Quantum Chem.* **1984**, *25*, 1123–1134.

(22) Lazzeretti, P.; Malagoli, M.; Zanasi, R. In *Nuclear Magnetic Shieldings and Molecular Structure*; Tossell, J. A., Ed.; Springer Netherlands: Dordrecht, 1993; pp 163–190.

(23) Bader, R. F. W. *Atoms in Molecules: A Quantum Theory*; The International Series of Monographs on Chemistry 22; Clarendon Press ; Oxford University Press: Oxford [England] : New York, 1994.

(24) Wilson, P. J.; Bradley, T. J.; Tozer, D. J. Hybrid Exchange-correlation Functional Determined from Thermochemical Data and *Ab Initio* Potentials. *J. Chem. Phys.* **2001**, *115*, 9233–9242.

(25) Dunning, T. H. Gaussian Basis Sets for Use in Correlated Molecular Calculations. I. The Atoms Boron Through Neon and Hydrogen. *J. Chem. Phys.* **1989**, *90*, 1007–1023.

(26) Flaig, D.; Maurer, M.; Hanni, M.; Braunger, K.; Kick, L.; Thubauville, M.; Ochsenfeld, C. Benchmarking Hydrogen and Carbon NMR Chemical Shifts at HF, DFT, and MP2 Levels. *J. Chem. Theory Comput.* **2014**, *10*, 572–578.

(27) Zanasi, R.; Lazzeretti, P.; Malagoli, M.; Piccinini, F. Molecular Magnetic Properties

within Continuous Transformations of Origin of the Current Density. *J. Chem. Phys.* **1995**, *102*, 7150–7157.

(28) Zanasi, R. Coupled Hartree-Fock Calculations of Molecular Magnetic Properties Annihilating the Transverse Paramagnetic Current Density. *J. Chem. Phys.* **1996**, *105*, 1460–1469.

(29) Havenith, R. W.; Fowler, P. W. Ipsocentric Ring Currents in Density Functional Theory. *Chem. Phys. Lett.* **2007**, *449*, 347–353.

(30) Havenith, R. W.; Meijer, A. J.; Irving, B. J.; Fowler, P. W. Comparison of Ring Currents Evaluated Consistently at Density Functional and Hartree-Fock Levels. *Mol. Phys.* **2009**, *107*, 2591–2600.

(31) Soncini, A.; Teale, A. M.; Helgaker, T.; De Proft, F.; Tozer, D. J. Maps of Current Density Using Density-functional Methods. *J. Chem. Phys.* **2008**, *129*, 074101.

(32) Frisch, M. J.; Trucks, G. W.; Schlegel, H. B.; Scuseria, G. E.; Robb, M. A.; Cheeseman, J. R.; Scalmani, G.; Barone, V.; Mennucci, B.; Petersson, G. A.; et al., Gaussian 09, Revision D.01, Gaussian, Inc., Wallingford CT. 2013.

(33) Lazzeretti, P.; Malagoli, M.; Zanasi, R. *Technical Report on Project "Sistemi Informatici e Calcolo Parallelo"*; Research Report 1/67, 1991.

(34) Carion, R.; Champagne, B.; Monaco, G.; Zanasi, R.; Pelloni, S.; Lazzeretti, P. Ring Current Model and Anisotropic Magnetic Response of Cyclopropane. *J. Chem. Theory Comput.* **2010**, *6*, 2002–2018.

(35) Ligabue, A.; Pincelli, U.; Lazzeretti, P.; Zanasi, R. Current Density Maps, Magnetizability, and Nuclear Magnetic Shielding Tensors for Anthracene, Phenanthrene, and Triphenylene. *J. Am. Chem. Soc.* **1999**, *121*, 5513–5518.

Accepted Version of J. Phys. Chem. A 2019, 123, 1558 doi: 10.1021/acs.jpca.8b10836

(36) Monaco, G.; Scott, L. T.; Zanasi, R. Magnetic Euripi in Corannulene. *J. Phys. Chem. A* **2008**, *112*, 8136–8147.

(37) Coddington, E. A.; Levinson, N. *Theory of Ordinary Differential Equations*; McGraw-Hill, New York, 1955.

(38) Reyn, J. W. Classification and Description of the Singular Points of a System of Three Linear Differential Equations. *Z. Angew. Math. Phys.* **1964**, *15*, 540–557.

(39) Ferraro, M.; Lazzeretti, P.; Viglione, R.; Zanasi, R. Understanding Proton Magnetic Shielding in the Benzene Molecule. *Chem. Phys. Lett.* **2004**, *390*, 268–271.

(40) Pelloni, S.; Faglioni, F.; Zanasi, R.; Lazzeretti, P. Topology of Magnetic-field-induced Current-density Field in Diatropic Monocyclic Molecules. *Phys. Rev. A* **2006**, *74*, 012506–1–8.

(41) Pelloni, S.; Lazzeretti, P.; Zanasi, R. Spatial Ring Current Model of the [2.2]Paracyclophane Molecule. *J. Phys. Chem. A* **2007**, *111*, 3110–3123.

(42) Pelloni, S.; Lazzeretti, P.; Zanasi, R. Topological Models of Magnetic Field Induced Current Density Field in Small Molecules. *Theor. Chem. Acc.* **2009**, *123*, 353–364.

(43) Pelloni, S.; Lazzeretti, P.; Zanasi, R. Induced Orbital Paramagnetism and Paratropism in Closed-Shell Molecules. *J. Phys. Chem. A* **2009**, *113*, 14465–14479.

(44) Pelloni, S.; Lazzeretti, P.; Monaco, G.; Zanasi, R. Magnetic-field Induced Electronic Anapoles in Small Molecules. *Rendiconti Lincei* **2011**, *22*, 105–112.

(45) Pelloni, S.; Lazzeretti, P.; Zanasi, R. Assessment of σ-Diatropicity of the Cyclopropane Molecule. *J. Phys. Chem. A* **2007**, *111*, 8163–8169.

(46) Tavger, B. A.; Zaitsev, V. M. Magnetic Symmetry of Crystals. *Sov. Phys. JETP* **1956**, *3*, 430–436.

(47) Monaco, G.; Zanasi, R. On the Additivity of Current Density in Polycyclic Aromatic Hydrocarbons. *J. Chem. Phys.* **2009**, *131*, 044126.

(48) Jameson, C. J.; Buckingham, A. D. Molecular Electronic Property Density Functions: The Nuclear Magnetic Shielding Density. *J. Chem. Phys.* **1980**, *73*, 5684–5692.

(49) Jameson, C. J.; Buckingham, A. D. Nuclear Magnetic Shielding Density. *J. Phys. Chem.* **1979**, *83*, 3366–3371.

(50) Pelloni, S.; Monaco, G.; Della Porta, P.; Zanasi, R.; Lazzeretti, P. Delocalized Currents without a Ring of Bonded Atoms: Strong Delocalized Electron Currents Induced by Magnetic Fields in Noncyclic Molecules. *J. Phys. Chem. A* **2014**, *118*, 3367–3375.

(51) Monaco, G.; Porta, P. D.; Jabłoński, M.; Zanasi, R. Topology of the Magnetically Induced Current Density and Proton Magnetic Shielding in Hydrogen Bonded Systems. *Phys. Chem. Chem. Phys.* **2015**, *17*, 5966–5972.

(52) Lee, C. J.; Kang, Y.-M.; Cho, K.-H.; No, K. T. A Robust Method for Searching the Smallest Set of Smallest Rings with a Path-included Distance Matrix. *P. Natl. Acad. Sci. USA* **2009**, *106*, 17355–17358.

(53) Medvedev, N. The Algorithm for Three-dimensional Voronoi Polyhedra. *J. Comput. Phys.* **1986**, *67*, 223–229.

(54) Epstein, S. T. Gauge Invariance, Current Conservation, and GIAO's. *J. Chem. Phys.* **1973**, *58*, 1592–1595.

(55) Sambe, H. Properties of Induced Electron Current Density of a Molecule Under a Static Uniform Magnetic Field. *J. Chem. Phys.* **1973**, *59*, 555–555.

(56) Schmalz, T. G.; Norris, C. L.; Flygare, W. H. Localized Magnetic Susceptibility Anisotropies. *J. Am. Chem. Soc.* **1973**, *95*, 7961–7967.

Accepted Version of J. Phys. Chem. A 2019, 123, 1558 doi: 10.1021/acs.jpca.8b10836

(57) Corminboeuf, C.; Heine, T.; Seifert, G.; Schleyer, P. v. R.; Weber, J. Induced Magnetic Fields in Aromatic [n]-Annulenes—Interpretation of NICS Tensor Components. *Phys. Chem. Chem. Phys.* **2004**, *6*, 273–276.

(58) Schleyer, P. v. R.; Maerker, C.; Dransfeld, A.; Jiao, H.; van Eikema Hommes, N. J. R. Nucleus-Independent Chemical Shifts: A Simple and Efficient Aromaticity Probe. *J. Am. Chem. Soc.* **1996**, *118*, 6317–6318.

(59) Fallah-Bagher-Shaidaei, H.; Wannere, C. S.; Corminboeuf, C.; Puchta, R.; Schleyer, P. v. R. Which NICS Aromaticity Index for Planar π Rings Is Best? *Org. Lett.* **2006**, *8*, 863–866.

(60) Lukins, P. B.; Laver, D. R.; Buckingham, A. D.; Ritchie, G. L. D. Cotton-Mouton Effect, Magnetic Anisotropy and Charge Distribution of Cyclopropane. *J. Phys. Chem.* **1985**, *89*, 1309–1312.

Accepted Version of J. Phys. Chem. A 2019, 123, 1558 doi: 10.1021/acs.jpca.8b10836

Graphical TOC Entry